Received: 2 April 2021 | Revised: 10 June 2021 | Accepted: 21 June 2021

DOI: 10.1111/iwj.13652

ORIGINAL ARTICLE

IWJ WILEY

A novel atmospheric-pressure air plasma jet for wound healing

Peng Guo[1] | Yang Liu[2] | Juan Li[3] | Nan Zhang[2] | Ming Zhou[4] | Yi Li[3] | Guozhu Zhao[3] | Ning Wang[4] | Aiguo Wang[2] | Yupeng Wang[3] | Fujin Wang[2] | Liping Huang[4]

[1]Department of Gastroenterological Surgery, Peking University People's Hospital, Beijing, China

[2]Department of Comparative Medicine, Laboratory Animal Center, Dalian Medical University, Dalian, Liaoning, China

[3]Yantai Healing Technology Co. Ltd, Yantai, Shandong, China

[4]Department of Rehabilitation Medicine, the First Medical Center, Chinese PLA General Hospital, Beijing, China

Correspondence
Liping Huang, Department of Rehabilitation Medicine, the First Medical Centre, Chinese PLA General Hospital, Beijing 100853, P. R. China.
Email: ping-online@163.com

Fujin Wang, Laboratory Animal Centre, Dalian Medical University, Dalian, Liaoning 116044, P. R. China.
Email: wangfujin2000@163.com

Yupeng Wang, Yantai Healing Technology Co. Ltd., Yantai, Shandong 264006, P. R. China.
Email: 13901237491@139.com

Funding information
Yantai Healing Technology Co. Ltd.

Abstract

Current low-temperature plasma (LTP) devices essentially use a rare gas source with a short working distance (8 to 20 mm), low gas flow rate (0.12 to 0.3 m^3/h), and small effective treatment area (1-5 cm^2), limiting the applications for which LTP can be utilised in clinical therapy. In the present study, a novel type of LTP equipment was developed, having the advantages of a free gas source (surrounding air), long working distance (8 cm), high gas flow rate (10 m^3/h), large effective treatment area (20 cm^2), and producing an abundance of active substances (NOγ, OH, N_2, and O), effectively addressing the shortcomings of current LTP devices. Furthermore, it has been verified that the novel LTP device displays therapeutic efficacy in terms of acceleration of wound healing in normal and Type I diabetic rats, with enhanced wound kinetics, rate of condensation of wound area, and recovery ratio. Cellular and molecular analysis indicated that LTP treatment significantly reduced inflammation and enhanced re-epithelialization, fibroblast proliferation, deposition of collagen, neovascularization, and expression of TGF-β, superoxide dismutase, glutathione peroxidase, and catalase in Type I diabetic rats. In conclusion, the novel LTP device provides a convenient and efficient tool for the treatment of clinical wounds.

KEYWORDS

low-temperature plasma (LTP), novel LTP device, type I diabetes, wound healing

Key Messages

- currently, LTP is an effective method for promoting wound healing
- the novel LTP device in this study addresses the shortcomings of current LTP devices
- the promotion effect of LTP on wound healing is a combination of plasma-active substances and thermal

Peng Guo and Yang Liu contributed equally to this work.

1 | INTRODUCTION

Plasma is regarded as the fourth state of matter, distinct from solids, liquids, and gases, generated when sufficient energy is provided to a gas. Such energy can be provided by electricity, radiation, or thermal or chemical means, alone or in combination.[1] Of these, thermal energy and electricity are common methods for the excitation of plasma. In nature, large quantities of plasma are generated at temperatures of up to 15 million degrees within the sun.[2] However, the very high temperatures required to excite plasma by thermal energy alone limits its applicability for clinical treatments. Therefore, low-temperature plasmas (LTPs) produced by ionised gas via high-voltage alternating current (AC) provides opportunities for the usage of plasma in the biomedical field.

Studies of LTP technology in medicine can be traced back to the beginning of the last century.[3] However, due to a lack of understanding of the nature of plasma and the weak technical capabilities at that time, groundbreaking studies of plasma could not be conducted, and major breakthroughs were not achieved. Laroussi et al were the first to use atmospheric pressure cold plasma in 1996 to achieve bacterial inactivation.[4] Since then, related research reports have emerged in the literature, studies developing from relatively simple in vitro disinfection to in vivo experiments and even clinical applications. Current studies of LTP, from exploratory research to in-depth investigations of its mechanisms in medical applications and technologies have achieved new milestones with encouraging results in a number of medical fields, such as healing of the skin,[5] treatment of the oral cavity[6] and cancer.[7]

A variety of LTP devices have been developed and tested for different medical applications. In general, there are two categories of LTP devices: those that undergo direct discharge and those that are indirect, namely, dielectric barrier discharge (DBD) or atmospheric pressure plasma jet (APPJ) devices. However, few LTP devices have been certified for medical usage. Currently, three plasma devices have been certified for medical purposes: the kINPen® MED (INP Greifswald/Neoplas Tools Co., Ltd., Greifswald, Germany), an APPJ, principally for the treatment of non-healing wounds and skin diseases caused by pathogens[8,9]; the PlasmaDerm® VU-2010 (CINOGY Technologies GmbH, Duderstadt, Germany), a DBD source, CE-certified in Germany by MEDCERT with good therapeutic effects on the chronic venous ulcers of lower limbs,[10,11] and the SteriPlas (Adtec Ltd., London, United Kingdom), used principally for the treatment of chronic and acute wounds, resulting in a reduction of microbial load.[10] However, the LTP devices currently used clinically essentially use a rare gas source with a short working distance (8 to 20 mm), low gas flow rate (0.12-0.3 m^3/h), and small effective treatment area (1-5 cm^2), limiting potential clinical applications for LTP.

In the present study, a novel type of LTP device was developed which had a free gas source (air), a long working distance (8 cm), high gas flow rate (10 m^3/h), and a large effective treatment area (20 cm^2), effectively addressing the shortcomings of current LTP devices. Furthermore, it was verified that the new LTP equipment provides accelerated wound healing in normal and Type I diabetic rats. The prototype of the LTP device has been registered and certified as a medical instrument by the China Institute of Food and Drug Control (registration number: QH20200272). The equipment and related methods for applications using this LTP instrument have been patented (CN201610272491.4; European patent No. 3446749). The device will broaden the potential range of clinical therapeutic applications for plasma.

2 | MATERIALS AND METHODS

2.1 | Low-temperature plasma (LTP) device

In this study, a specially designed LTP jet device driven by high-voltage AC, is reported. As shown in Figure 1A, the device consists of an LTP jet generator, an air supply system, and a high-voltage AC power supply. The LTP jet generator comprises two copper electrodes in a coaxial layout. The diameter of the inner solid positive electrode is 8 mm and the inner diameter of the outer hollow cylinder of the negative electrode is 25 mm. The two electrodes are attached at the base with an insulator. Except for the basal insulator component, the effective length of the inner electrode is 15.5 mm and the outer electrode is 47 mm. The distance between the tip of the inner electrode and the nozzle of the outer electrode is 31.5 mm. There is an 8.5 mm gap between the positive and negative electrodes. The middle ring cavity of two electrodes forms a gas channel. The air supply system injects surrounding air into the gas channel from a pipeline adjoining the insulation. There is an annular device situated at an oblique angle with pores at a 45° angle, which is connected to the air pipeline, ensuring air enters the gas channel evenly. Airflow at a rate of 10 m^3/h was achieved, representing an airflow velocity at the nozzle of 3 to 4 m/s. Plasma is generated by ionisation of the air between the two electrodes, with active species in the plasma propelled from the generator nozzle by airflow. The prototype LTP equipment is

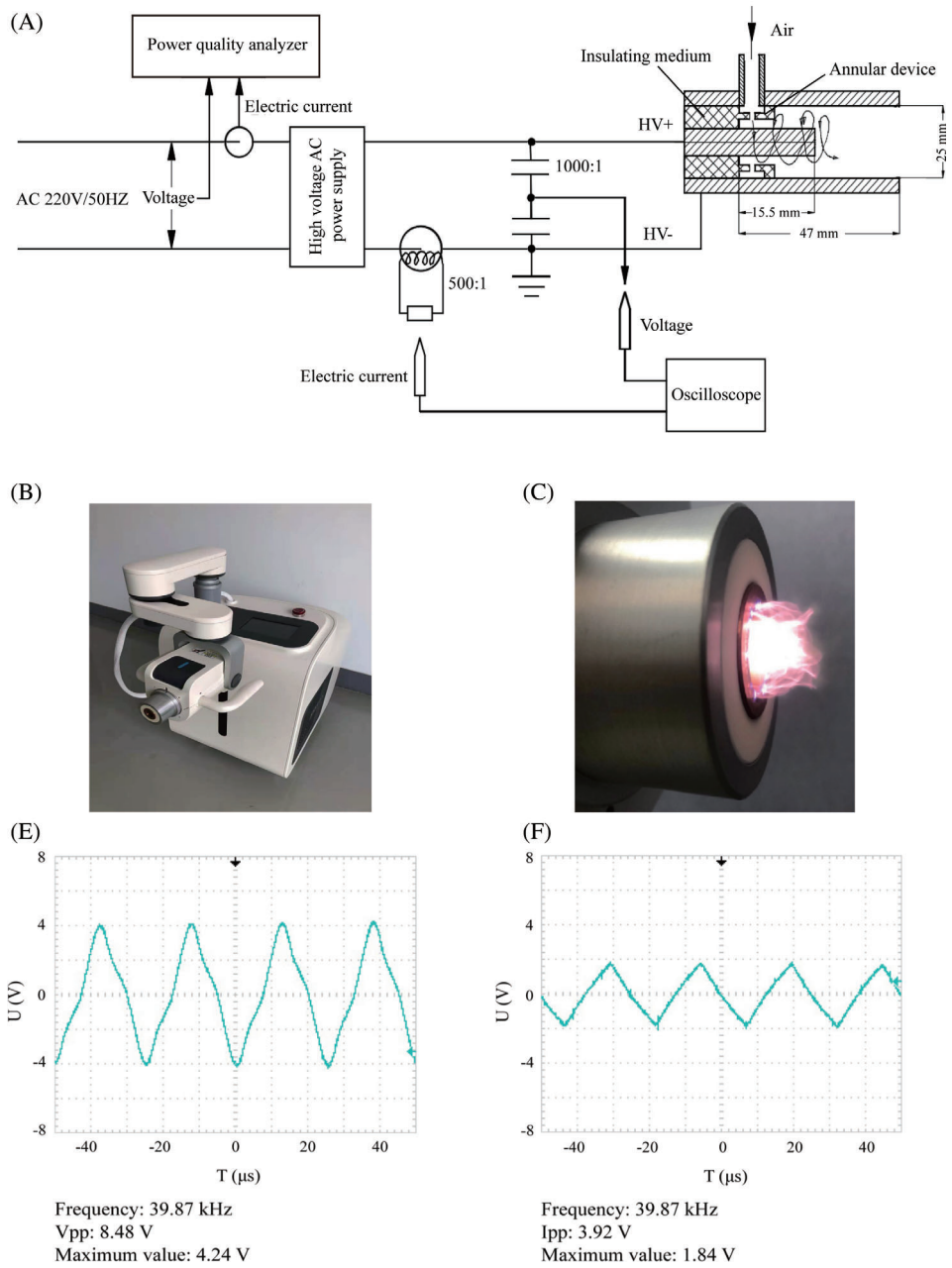

FIGURE 1 Schematic illustration of the novel LTP device and electrical measurement system. A, Schematic illustration of the LTP jet equipment. B, The prototype of the LTP equipment. C, Plasma jet generated by the LTP equipment. Voltage (ratio, 1000:1) and current (ratio, 500:1) waveforms of the AC high-voltage power supply. D, The plasma load peak-to-peak voltage (Vpp). E, The load peak-to-peak current (Ipp)

displayed in Figure 1B while the plasma jet it generates is presented in Figure 1C.

2.2 | Measurement of physical property of the LTP device

A power quality analyser (Fluke 43B) was used to measure the input power of the high-voltage AC power supply system. Measurement of the output voltage and current waveform of the high-voltage AC power supply was performed using an oscilloscope (TDS 2024C, Tektronix). The temperature of LTP was determined using a thermometer (TES 1310 TYPE-K) at various vertical distances from the plasma nozzle.

2.3 | Measurement of chemical property of the LTP

To establish the characteristics of the plasma, a fully automated Langmuir probe detection system (Impedans Ltd.) was used to measure the plasma parameters in real-time. OES was performed to analyse the excited species using an optical emission spectrometer (Avasoec-ULS2048; Avantes) with a resolution of 0.5 nm, in which an optical fibre connected the slit adapter (OES side) to a collimating lens (measurement side) (Model 75-UV; WY Optics). The lens had a focal length of 10 mm and was used to receive collimated light with a diameter of approximately 5 mm. Data were obtained and analysed using AvaSoft 7.8 spectroscopy software. Further, to

determine the effective treatment area, the concentration of NO was measured as an indicator. We use a gas analyser (Testo 330-1 flue gas analyser) to detect the actual concentration of NO at flow rate of 10 m^3/h and a distance of 80 mm from the nozzle of the plasma generator with the temperature controlled to 43 ± 0.5°C.

2.4 | Measurement of ROS/RNS

Reactive oxygen/nitrogen species (ROS/RNS) measurements were performed using deionised water instead of tissue fluid from wounds because they easily dry out and it was not possible to obtain sufficient fluid after plasma treatment for species quantification. Although tissue fluid is different from deionised water, the primary component of fluids from wounds is water. Thus, the use of deionised water to mimic fluid from wounds was appropriate, allowing an assessment of the novel LTP device to generate H_2O_2 and NO_2^- over varying durations and distance from the water surface.

A 3.5 cm plate with 1 mL deionised water was placed 8 cm away directly below the nozzle of the LTP device, and the airflow rate was set as 6 m^3/h or 10 m^3/h. An Amplex Red hydrogen peroxide/peroxide assay kit (Invitrogen) was used to quantify the concentration of H_2O_2 in the LTP-treated deionised water. The samples were pipetted into the individual wells of a microplate containing Amplex Red stock solution and HRP stock solution then incubated at room temperature for 30 minutes in the dark. The presence of H_2O_2 was measured from the absorbance at 560 nm. As nitrite (NO_2^-) and nitrate (NO_3^-) are the final stable products of RNS, both were measured for the quantification of RNS production. Therefore, a nitrite/nitrate colorimetric assay kit (Beyotime) was used to measure the total quantity of NO_2^- and NO_3^-. The treated samples were pipetted into the individual wells of a microplate containing kit reagents. After development of the colour reaction, light absorbance (540 nm) was measured using a plate reader.

When treatment time is greater than 300 seconds, the evaporated water volume is over 75%. Therefore, the maximum irradiation time was set at 300 s. Considering the volume of evaporated water, the concentrations of ROS/RNS at each time point were calculated as following formula: measured concentration/(1-evaporated water [mL]).

2.5 | Wound healing in an animal model

2.5.1 | Animals

Eight-week-old male Wistar rats (200-230 g) (Liaoning Changsheng Biotechnology, China) were used in a diabetic wound healing animal model and 12-week-old male Wistar rats (400-500 g) for normal wound healing. The rats were maintained in a specific pathogen-free environment at a constant temperature of 22 ± 1°C and 55 ± 5% humidity within 12 hours light/dark cycle, and fed normal chow (12% calories as fat). Each rat was individually caged to prevent biting or fighting with other rats.

2.5.2 | Diabetic rat model

Streptozotocin (STZ) was used to induce Type I diabetes in rats, in which the islet β cells were thoroughly destroyed, causing an absolute lack of insulin. The model was induced using a single, relatively high dose (60 mg/kg) of STZ (dissolved in 0.1 M citrate buffer, pH 4) administered by intraperitoneal injection. Prior to the injection of STZ, the rats were fasted overnight but had free access to water to prevent dehydration. STZ was then administered the following morning with a recovery diet. A week after the injection of STZ, the blood glucose levels of the Type 1 diabetic rats were measured using a glucometer (590; Yuwell). A small incision was created on the rat tail using a surgical blade and the blood tested with a blood glucose test strip to monitor blood glucose levels. It was confirmed that the model of diabetes was established for rats in which glucose levels were higher than 16.7 mmol/L. Glucose levels were monitored on a daily basis during the experiment. Insulin was injected only when the glucose levels exceeded 27.6 mmol/L, to prevent the rats from becoming weak and suffering sudden death.

2.5.3 | Incisional wound model and wound treatment

The rats were anaesthetised using 3% isoflurane for surgery. The fur on the backs of the rats was shaved using an electric clipper after the rats went unconscious. A 3.5 cm^2 full-thickness round wound was created at the junction of the spine and the two leg joints. The normal and diabetic rats were randomly allocated into one of three groups, with 5 normal rats and 10 diabetic rats in each group: (1) the control group, in which wounds healed spontaneously without treatment; (2) hot-air treatment group, in which an air heater was used to treat the wounds; (3) LTP-treated group, in which a new type of LTP device was used to treat the wounds. Treatment was performed for 3 minutes once per day after creating the incision until the wound had healed. During the entire treatment process, the temperature of the wound and around the skin surface was controlled to 43 ± 0.5°C.

2.5.4 | Skin temperature measurement

The temperature of the wound and around the skin surface were real-time monitored using an infrared thermal imager Fluke Ti200 (Fluke Co., Ltd., USA) with a measurement range of −20°C to +650°C, an accuracy of ±2°C or 2% of the measurement, MRTD (Minimum Resolvable Temperature Difference) ≤ 0.075°C, in a controlled room at a temperature of 25.0°C and a humidity of 60%. By using the centre of wound as the temperature-measuring point, the thermogram was real-time recorded and the data were saved into the computer. The high-temperature alarm was set at 43.5°C. This kind of detection is non-invasive, and not harmful to rat bodies.

2.6 | Wound healing analysis

2.6.1 | Wound kinetics and calculation

The kinetics of wound healing were recorded using a camera every day after creating the wounds (Day 0) until the wounds had healed. A ruler was placed beside the wound as a scale with which to calculate wound area and compare sizes for various conditions. The daily wound area was calculated using image analysis software (ImageJ), in which the wound area ratio was defined as the ratio of wound area at time t, to the initial wound area, allowing quantification of the rate of wound healing, for evaluating healing efficacy. The wound area condensation rate (%) = residual wound area / initial wound area × 100%. The time for each wound on each rat to heal was recorded and the recovery rate for each group calculated.

2.6.2 | Sampling

The rats were euthanized with 20% chloral hydrate on Day 14, and then a piece of skin that included the wound and adjacent uninjured tissue was removed using scissors. Part of this tissue was used for histology and the remaining piece was cut into small pieces, each weighing approximately 20 mg, which were stored in liquid nitrogen for subsequent antioxidant testing. The tissue for histology was placed on filter paper and soaked in 4% paraformaldehyde for fixation.

2.6.3 | Haematoxylin and eosin (H&E) staining and quantification

Fixed skin tissue was gradually dehydrated using grads-alcohol, then embedded in paraffin. A microtome was then used to cut the tissue into 5 μm-thick sections. H&E staining was performed in accordance with standard protocols. ImageJ software was used to count the number of lymphocytes and fibroblasts in the H&E stained images (400 ×). The degree of re-epithelialization was based on a random selection of 5 fields of view of images from each group (400 ×). The degree of re-epithelization = (length of newly formed epidermal layer/length of wound between its edges) × 100%.

2.6.4 | Masson's trichrome staining and quantification

Masson's trichrome staining was used to detect maturation of the connective tissue. Red staining represents keratin and muscle fibres and blue represents collagen. Light red or pink represents the cytoplasm and dark brown or black represents cell nuclei. The depth and organisation of blue staining can differentiate the maturity of the collagen fibres. After tissue sectioning, Masson's trichrome staining was performed in accordance with standard protocols (Servicebio). The levels of collagen deposition were quantified using ImageJ software by calculating five random fields from each sample by light microscopy (400 ×).

2.6.5 | Immunohistochemical staining and quantification

Tissue sections were analysed by immunohistochemistry (IHC). Slides were stained for antibodies against CD31, CK14, PCNA, and transforming growth factor-beta (TGF-β), the details of which are displayed in Table S1. The sections were first incubated with the antibodies at a dilution of 1:100 in PBS then incubated at room temperature for 1 hours. Staining was performed using a Discovery XT automated IHC/ISH slide staining system, using an UltraView Universal DAB detection kit (Ventana Medical System, Inc., Tucson) in accordance with the manufacturer's instructions.

To quantify the positively stained cells or tissue, five high-power fields (HPF) were randomly selected on each section at a magnification of 400 ×, from which staining intensity and the area of positive staining were analysed. This was achieved using the IHC Profiler plugin in ImageJ to automatically score the staining of sections.[12] Thus, the degree of angiogenesis, skin structural integrity, cell proliferation, and TGF-β expression were evaluated.

2.6.6 | Measurement of antioxidant concentration

Superoxide is very chemically active and has a very short life time, thus it is almost impossible to be measured

in vivo. To determine the effects of superoxide after treatment on wounds, we measured the ex vivo levels of SOD, CAT, and GPx to support the possibility that superoxide species is originally contained in the plasma or is synthesised during the plasma treatment. The liquid nitrogen-preserved tissue was homogenised in 1 × PBS and the concentrations of antioxidants in tissue homogenates were measured according to the kit instructions (Elabscience Biotechnology Co., Ltd.). The results were read by BIO-RAD xMark™ Microplate spectrophotometer (BIO-RAD, California, USA).

2.7 | Statistical analysis

Data are expressed as the mean ± standard deviation (SD). Statistical analyses were performed with one-way analysis of variance (ANOVA) followed by post-hoc *t*-test. The test was conducted for comparison of each experimental group in wound area calculation, score of histological staining, and measurement of antioxidant levels. P values <0.05 were considered significant.

3 | RESULTS

3.1 | Physical characterisation of the LTP device

The input power of the high-voltage AC power supply system was found to be 1000 W when connecting the current and voltage probes to the high-voltage AC power supply input (Figure 1A). The output voltage and current waveform of the high-voltage AC power supply was demonstrated in Figure 1D,E. The plasma load peak-to-peak voltage (Vpp) was 8.48 kV, load peak-to-peak current (Ipp) was 3.96 A, and frequency was 39.87 kHz.

The temperature of the plasma jet at the nozzle of the plasma generator was approximately 100°C and gradually decreased at increasing distances from the nozzle at an airflow rate of 10 m^3/h. The plasma temperature was approximately 43°C at a distance of 8 cm from the nozzle, consistent was the non-harmful treatment of skin. Therefore, subsequent experiments were conducted at this distance to identify the active substances in the plasma and the therapeutic efficacy in terms of acceleration of wound healing.

3.2 | Chemical characterisation of LTP

The plasma parameters in real-time are shown in Figure 2A. The electron temperature was 18.8 ev, ion current density was 649 mA/m^2, ion concentration was $2.08 \times 10^{17}/m^3$, Debye length was 55 μm, and saturation current was 0.00428 mA at an airflow rate of 10 m^3/h. These results indicate that there was an abundance of active substances within the plasma.

OES spectral data were collected for the hot-air (x = 9 cm) and LTP (x = 8 cm) devices, where "x" represents the treatment distance from the plasma jet nozzle. The temperature was limited to 43 ± 0.5°C. The OES spectral range was 200 to 400 nm for the ultraviolet (UV) light (Figure 2B) and 680 to 900 nm for visible light (Figure 2C). The results demonstrated that the intensities of NOγ, OH, N_2, and O were considerably higher in the LTP device compared with the hot-air device, in which active substances were barely detectable. This indicates that the excitation process in the LTP device created an abundance of active substances, mainly RNS and ROS. The effective area of tissue able to be treated was determined from the concentration of NO at various radial positions over the cross-section of the plasma jet. Using the experimental conditions described above, the concentration of NO within the centre of the plasma jet was 250 ppm, decreasing at lateral positions from the centre point. A concentration of 200 ppm (80% of the maximum value) was deemed the minimum considered to be fully effective. This value was achieved at a radius of 2.5 cm from the centre of the jet and, thus, the effective treatment area was calculated to be approximately 20 cm^2.

3.3 | Measurement of airflow rate, distance, and time effect of LTP on RNS and ROS

RNS and ROS are recognised as the principal active components in plasma that accelerate wound healing. To determine the appropriate conditions for treating wounds using an LTP device, the effects of distance and time on the concentration of RNS and ROS in LTP-treated deionised water were established. The results of NO_2^- and NO_3^- in deionised water treated with the LTP device at different distances and time points indicated that the concentration of nitrite/nitrate increased gradually with decreased distance (Figure 3A) and increased time (Figure 3B). Consistently, the trend of H_2O_2 concentration in deionised water treated with the LTP device was similar to that of nitrite/nitrate (Figure 3C,D). At the same time or distance, a higher content of H_2O_2 and nitrite/nitrate was produced in the LTP-treated deionised water with an airflow rate of 10 m^3/h group than that with an airflow rate of 6 m^3/h group. These results suggest that the active components in LTP can react with deionised water and produce free radicals and the

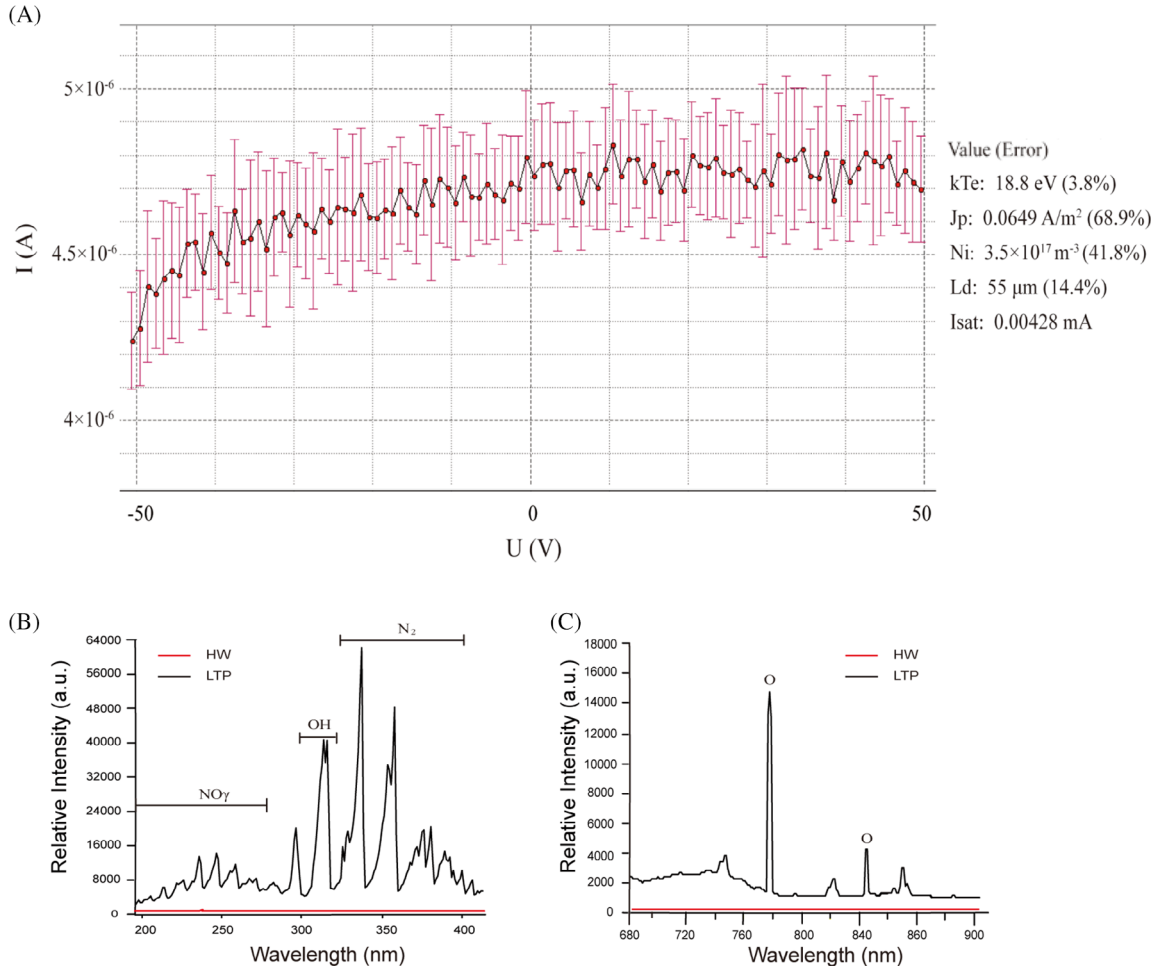

FIGURE 2 Parameters and OES spectral analysis of LTP. A, Parameters of the plasma measured by the Langmuir probe detection system in real-time. Isat, saturation current; Jp, Ionic current density; kTe, electron temperature; Ld, Debye length; Ni, ion concentration. B, Ultraviolet (UV) range (280-400 nm). C, Visible range (680-900 nm)

proportional relationship between ROS/RNS amount and airflow rate. As open wound tissue contains an abundance of extravasate, the results indicate that LTP is effective in inducing biological effects in wounds. After consideration of the intolerance of rat skin to high temperature, wounds were treated with the LTP device at a distance of 8 cm from the plasma jet nozzle for 3 minutes, with the temperature controlled to 43 ± 0.5°C.

3.4 | Effect of LTP on wound healing in normal rats

The kinetics of wound healing over time indicated that healing was considerably faster in the LTP-treated group than that in the hot air treatment and control groups (Figure 4A), with substantial differences in wound area and morphology. This was also reflected in the daily wound area condensation rate (Figure 4B). Furthermore, the wound recovery ratio indicated that recovery from wounds was significantly faster in the LTP-treated group than that in the hot-air treatment and control groups (Figure 4C). This indicates that LTP treatment significantly accelerates the wound healing process. It should also be noted that, although there was no statistical difference between the hot-air treatment groups and control group in terms of wound kinetics, the daily wound area condensation rate and wound recovery ratio were superior in the hot-air-treated group than in the control group, especially in the later stages of the healing process. This indicates that hyperthermia may promote wound healing.

3.5 | Effects of LTP on wound healing in diabetic rats

The same trend was observed in Type 1 diabetic rats, that is, LTP treatment significantly accelerated the wound healing process in comparison with the hot-air treatment

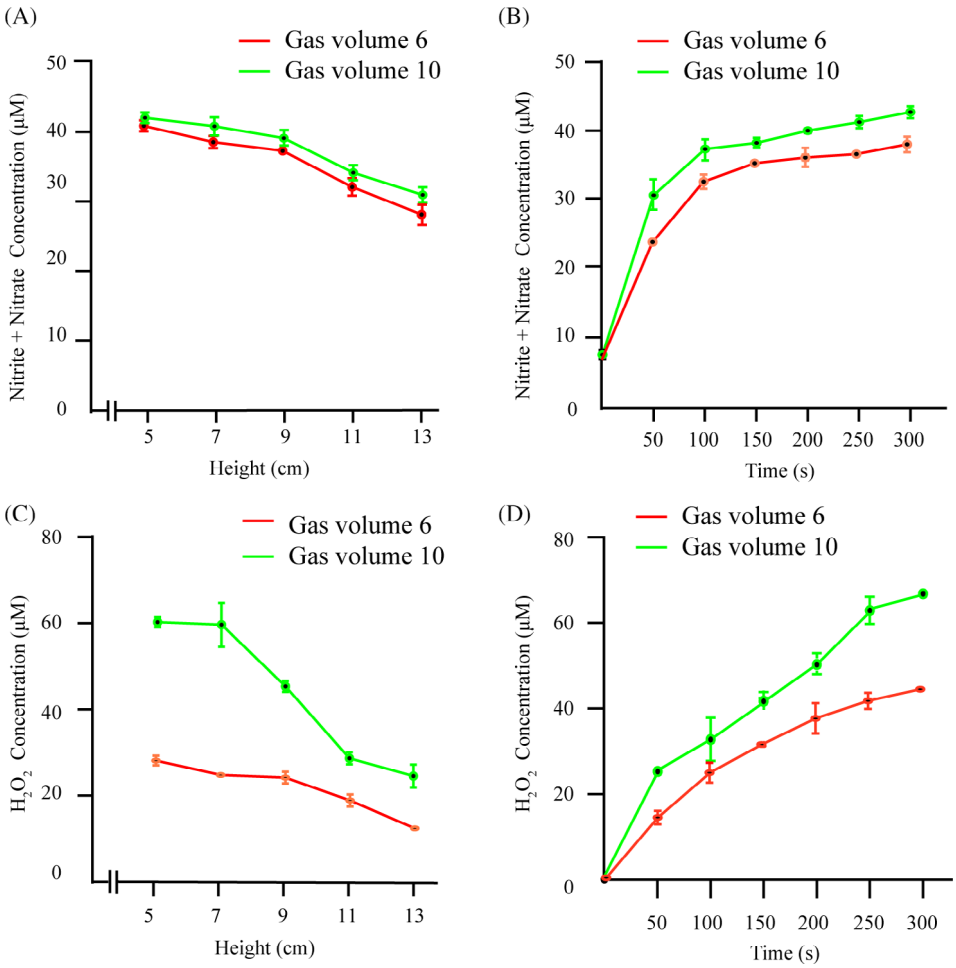

FIGURE 3 Concentrations of RNS and ROS in deionised water treated with the LTP device at various distances, time points and airflow rates. A,C, Changes in nitrite/nitrate or H_2O_2 concentration, at various distances and airflow rates after treatment for 3 minutes. B,D, Changes in nitrite/nitrate or H_2O_2 concentration at various time points and airflow rates after treatment at a distance of 8 cm. n = 3

and control groups, as reflected in wound kinetics (Figure 5A), daily wound area condensation rate (Figure 5B), and wound recovery ratio (Figure 5C). Interestingly, the hot-air treatment group demonstrated significantly faster healing than the control group, especially in the later stages of the healing process (Figure 5A-C). The results confirm that hyperthermia affects the healing process.

3.6 | Histological analysis

3.6.1 | Haematoxylin and Eosin (E&E) Staining

In agreement with wound kinetics data, substantial differences in wound area and morphology were observed at approximately Day 15 (Figure 5A). Therefore, the results at Day 14 were used for further histological analysis in the wounds of diabetic rats, in which significant differences between the control group and the other two groups were observed (Figure 5B). From H&E analysis, the re-epithelialization process was found to be faster and the skin structure was more complete in the LTP-treated group compared with the hot-air-treated or control groups (Figure 6A-C), and superior in the hot-air treated group than the control group (Figure 6A,B). These results were further reflected in the quantification of epithelial thickness and re-epithelialization, although there were no statistical differences between the hot-air-treated group and the other two groups (Figure 6D,E). Additionally, inflammatory cell infiltration and increased granulation tissue were observed in the dermis. Therefore, ImageJ was used to count the numbers of lymphocytes and fibroblasts. The results indicated that the infiltration of inflammatory cells was slightly but significantly lower in the hot-air treatment and LTP-treated groups compared with the control group (Figure 6F,G). The numbers of fibroblasts were significantly higher in the LTP-treated group compared with the control group. The mean number of fibroblasts in the hot-air-treated group was between the other two groups, for which there was no statistical difference observed. The results above indicate that, after LTP treatment, epithelial regeneration was accelerated, inflammation was reduced, and the proliferation of fibroblasts enhanced. Hot-air treatment also significantly reduced inflammation.

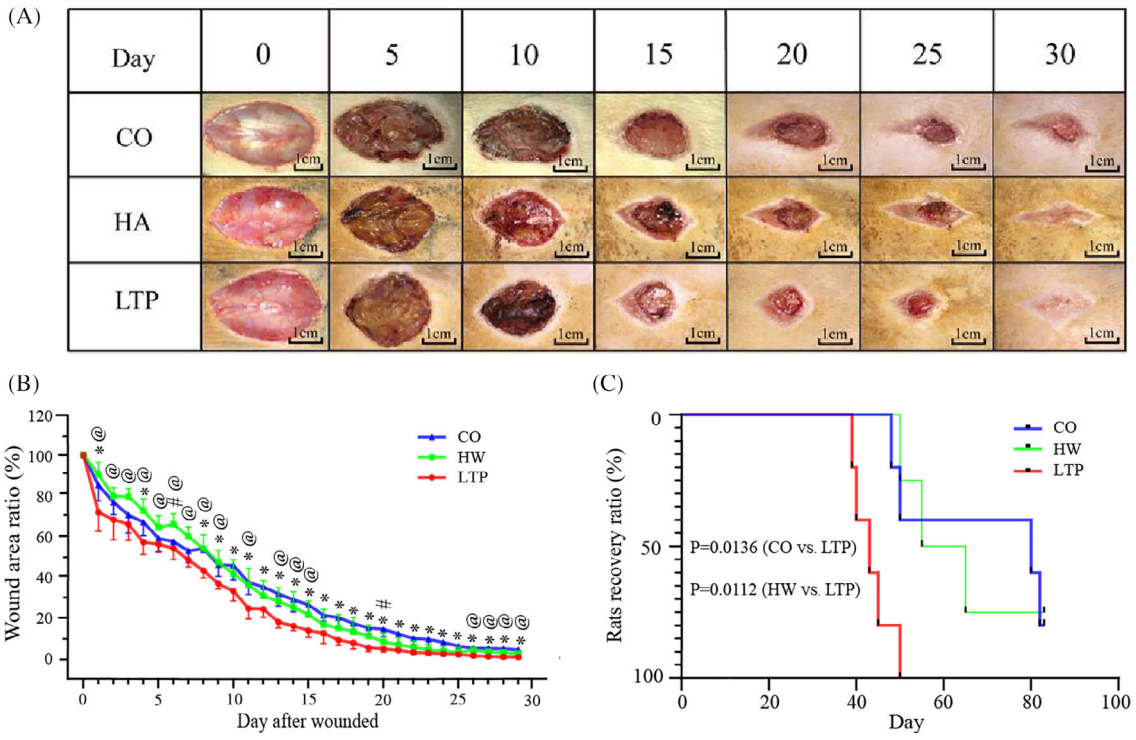

FIGURE 4 LTP treatment accelerates wound healing in normal rats. A, Wound healing kinetics on various days during the wound healing process. B, Daily wound area condensation rate during wound healing. C, Wound recovery ratio. CO, control group; HA, hot-air treatment group; LTP, LTP treatment group; *LTP versus CO ($P < .05$); # HW versus CO ($P < .05$); @ LTP versus HW ($P < .05$). n = 5

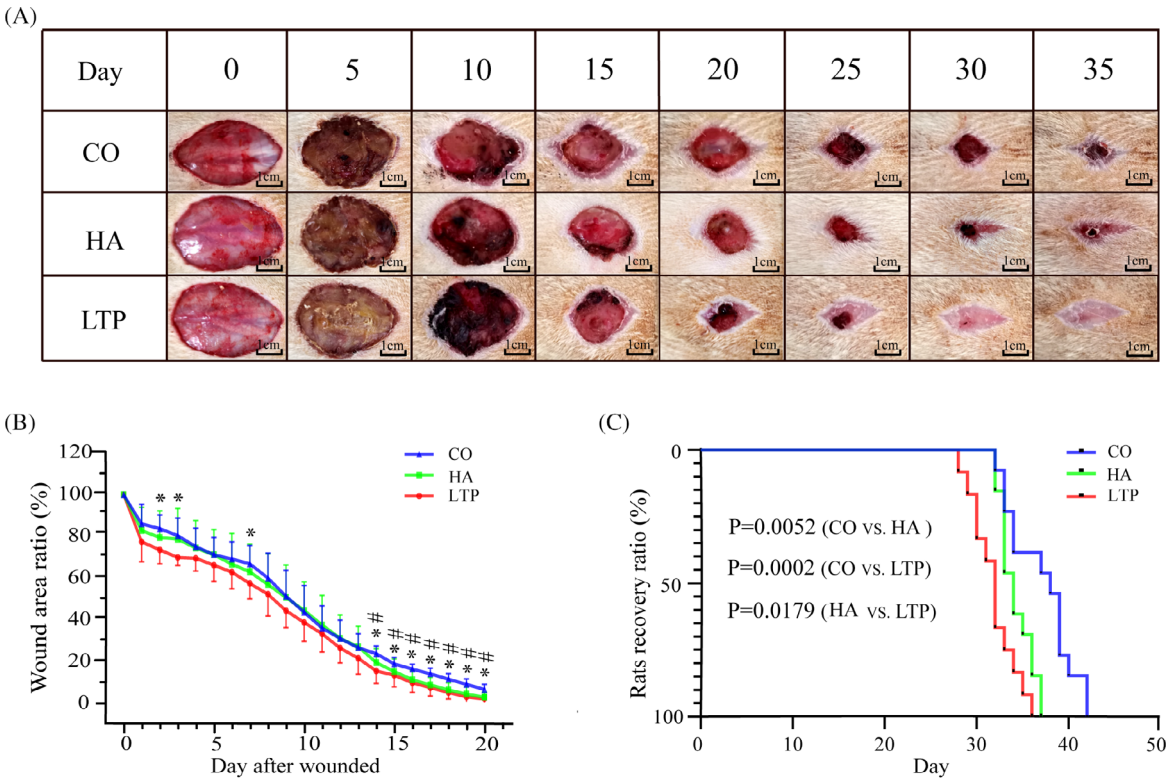

FIGURE 5 LTP treatment accelerates wound healing in Type I diabetic rats. A, Wound healing kinetics over time during wound healing. B, Daily wound area condensation rate during wound healing. C, Wound recovery ratio

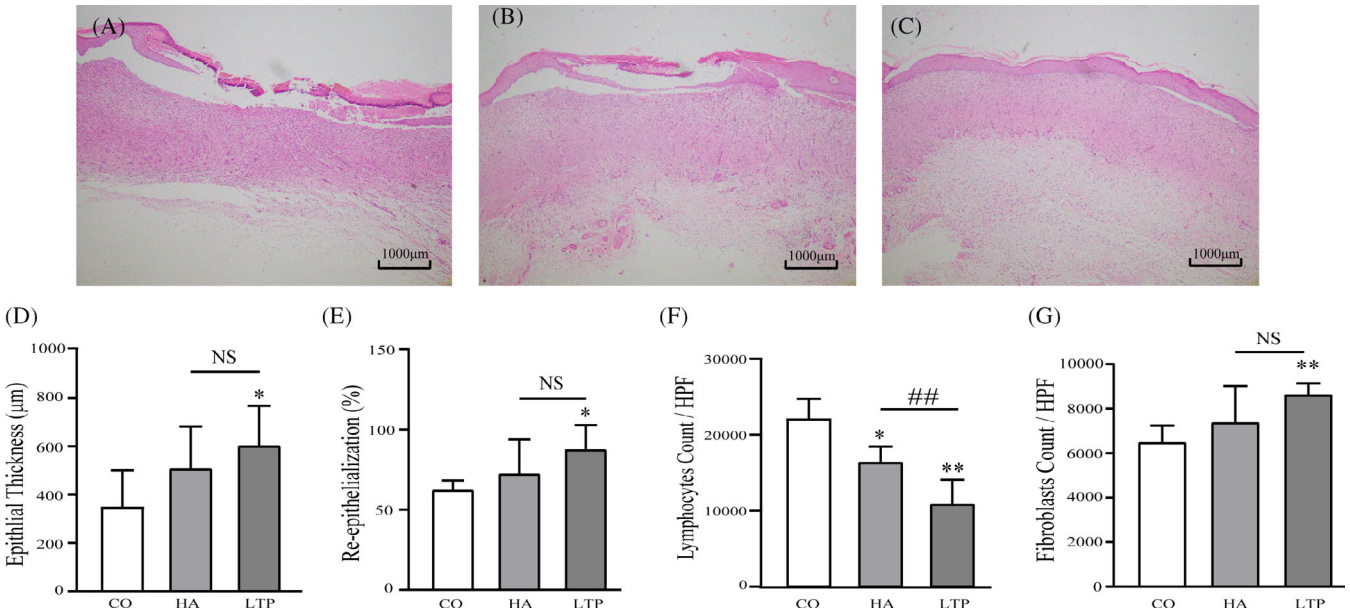

FIGURE 6 Haematoxylin and Eosin Staining analysis for Type I diabetic wounds. A, Control group. B, Hot-air treatment group. C, LTP treatment group. Quantification of the epithelial thickness (D), re-epithelialization (E), number of infiltrating lymphocytes (F), and number of fibroblasts (G). NS: no statistical differences; H&E magnification: 40×

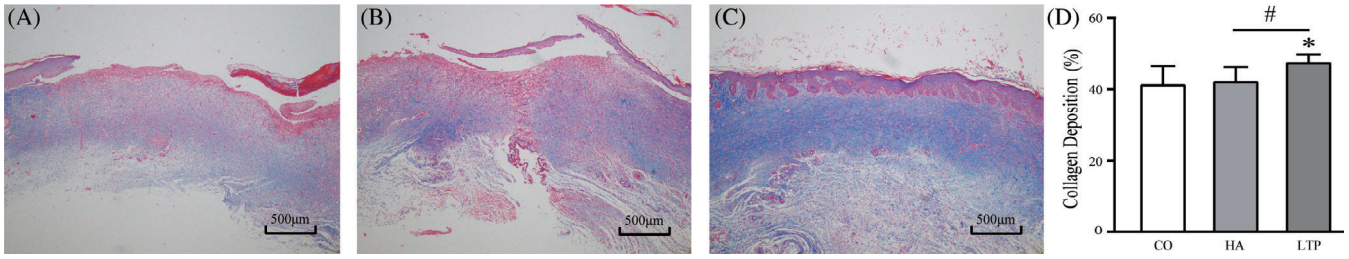

FIGURE 7 Masson's Trichrome Staining of Type I diabetic wounds. A, Control group. B, Hot-air treatment group. C, LTP treatment group. D, Quantification of collagen fibre staining intensity

3.6.2 | Masson's trichrome staining

Collagen deposition is a marker that reflects the wound healing process. Masson's trichrome stains collagen fibres blue and muscle fibres red. The intensity of blue staining represents the quantity and maturity of the collagen fibres. Masson's trichrome staining indicates that collagen fibres in the control and hot-air treatment groups are thick and with a disorderly arrangement (Figure 7A,B). In contrast, the collagen fibres in the LTP treatment group were arranged tightly and orderly, with a deeper coloration (Figure 7C). Quantification indicated that there was a significantly higher intensity of collagen fibres in the LTP-treatment group compared with the other two groups (Figure 7D). These results indicate that LTP treatment accelerated the wound healing process by enhancing collagen deposition.

3.6.3 | Immunohistochemical Staining

Immunohistochemical (IHC) staining was performed to measure the expression levels of CD31, CK14, PCNA, and TGF-β so that the wound healing process could be analysed. The number of CD31-positive cells, a marker for vascular endothelial cells, was considerably higher in the LTP-treated group than the other two groups (Figure 8A). This indicates that treatment with LTP clearly enhanced neovascularization. This was further reflected by the quantification of blood vessels (Figure 8A). CK14 staining, a marker of the basal layer of the epidermis, demonstrated that the integrity of the epithelial structure was gradually and significantly enhanced in the LTP and hot-air treatment groups, compared with the control group, although there was no statistical difference between the LTP and hot-air

treatment groups (Figure 8B). PCNA staining, a marker of cellular proliferation, indicated that the positively stained cells were mostly basal cells of the neonatal epidermis, indicating epithelial proliferation. Consistent with CK14 staining, PCNA-positive cells were slightly but significantly higher in number in the LTP and hot-air treatment groups compared with the control group, with no statistical difference between the LTP and hot-air treatment groups (Figure 8C). Additionally, a small number of PCNA-positive cells were observed in the dermal connective tissue, suggesting that there were no statistical differences between the experimental groups (data not shown). The intensity of staining for TGF-β, an important secretory cytokine that promotes wound healing, was slightly but significantly higher in the hot-air and LTP treatment groups compared with the control group (Figure 8D). This indicates that both plasma-active substances and higher temperature were able to promote the secretion of TGF-β in wounds.

3.7 | Measurement of antioxidant concentration

As the concentrations of SOD, GPx, and CAT are closely related to the scavenging of superoxide anions, which play an important role in inflammation in wound healing, we measured their concentrations in Type I diabetic wound tissues. The levels of SOD, GPx, and CAT were significantly elevated in both the hot-air and LTP treatment groups compared with the control group (Figure 9). However, although the LTP-treated group

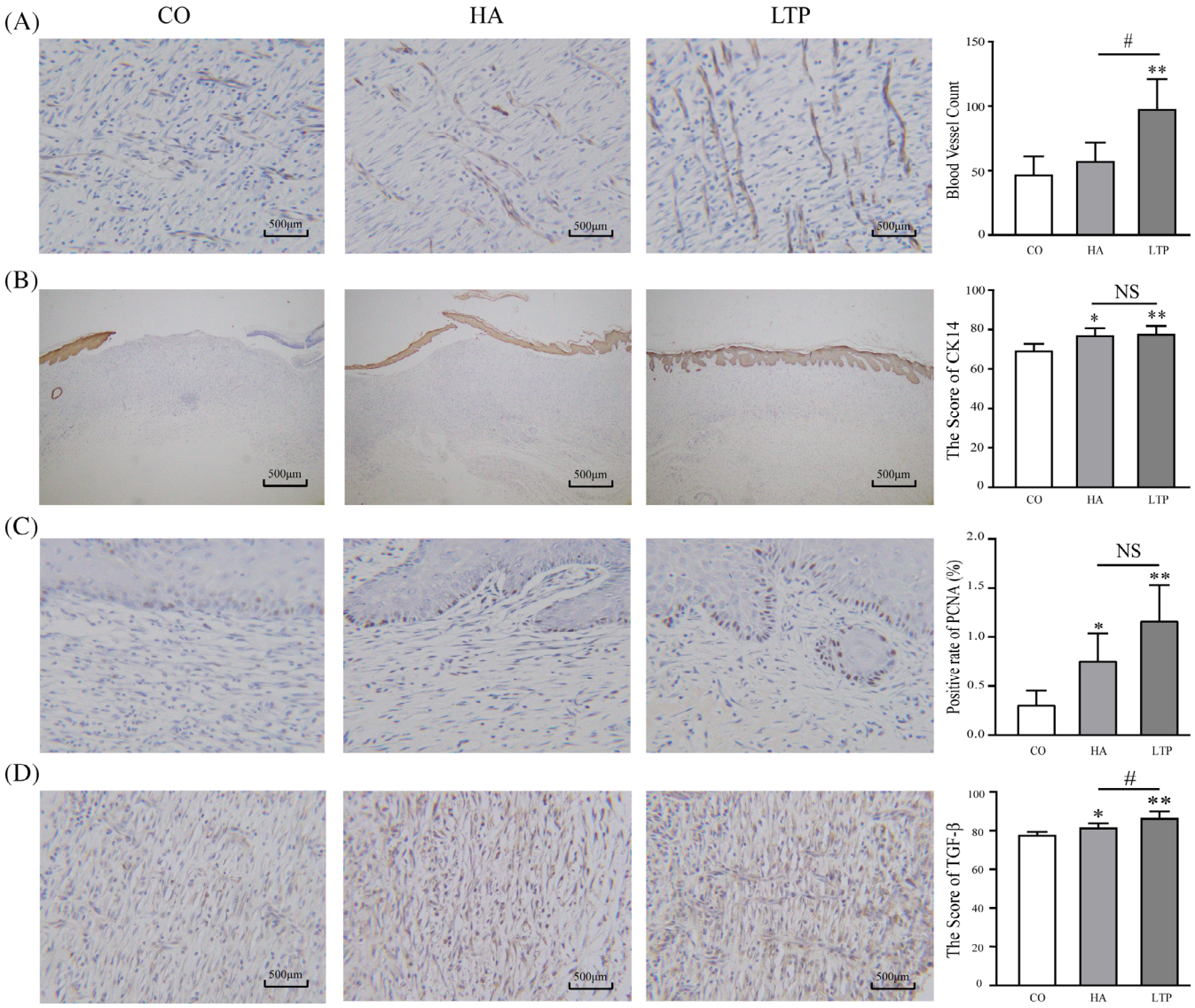

FIGURE 8 Immunohistochemical staining for Type I diabetic wounds. CD31 (A), CK14 (B), PCNA (C), TGF-β (D) staining (left panel) and relative quantification (right panel)

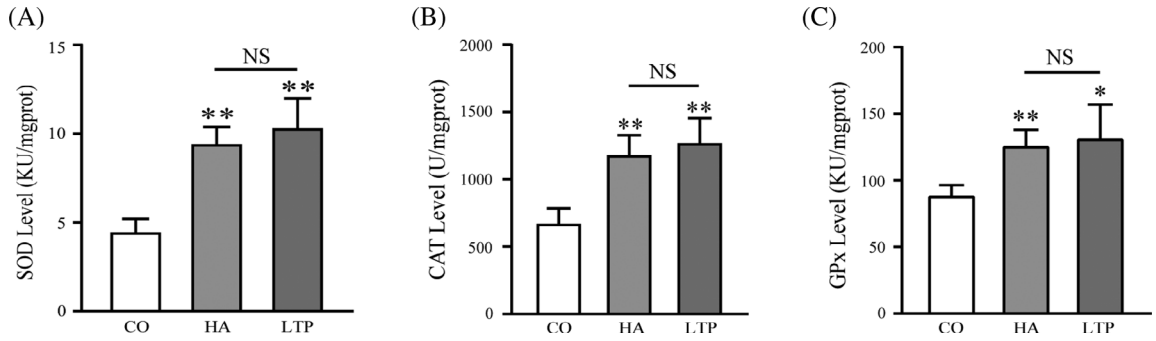

FIGURE 9 Antioxidant levels in Type I diabetic wounds. A, SOD, B, CAT, C, GPx. *$P < .05$ compared with control group

displayed slightly higher expression levels of SOD, GPx, and CAT compared with the hot-air treatment group, no statistical differences were observed between them (Figure 9). This indicates that both LTP and high temperature effectively reduced ROS/RNS and inflammation, resulting in accelerated wound healing via the promotion of antioxidant expression.

4 | DISCUSSION

It is worth noting that, compared with current plasma devices, the novel LTP device had many advantages, such as the free gas source, long working distance, high gas flow rate, and large effective treatment area. Firstly, current plasma devices used for wound treatments essentially utilise helium or argon as the gas source,[13,14] which is expensive and inconvenient. In comparison, the novel LTP device uses free and readily available surrounding air as a gas source. Secondly, compared with the current devices that require a treatment distance ranging from 8 to 20 mm between the plasma jet nozzle and body,[8,15] the new LTP device has a much longer working distance of up to 8 cm for which a curative effect is observed at a tolerable temperature, which is more practical for clinical applications. Thirdly, the gas flow rate of current plasma devices ranges from 0.12 to 0.3 m^3/h.[14,16] In contrast, the gas flow of the new LTP device was as high as 10 m^3/h, while producing more effective species. Fourthly, the effective treatment areas of the current plasma devices range from 1 to 5 cm^2.[3,13] The effective treatment area of the new LTP device is as high as 20 cm^2, greatly increasing the clinical treatment area. Therefore, the advantages of the new LTP device are effective in addressing the shortcomings of the current plasma devices and greatly expand the clinical and biomedical applications for plasma devices.

Wound healing is currently the principal application for plasma devices. In the present study, we have examined the efficacy of the novel LTP device in wound healing. The results demonstrate that the new LTP device accelerated wound healing by promoting the ratios of wound area condensation and wound recovery in both normal and diabetic rats compared with control groups (Figures 4 and 5). Further cellular and molecular examination demonstrated that the promotion of wound healing by the new LTP device was essentially driven by a reduction in inflammation (Figure 6), promotion of angiogenesis, epithelialization, and collagen deposition (Figures 6 and 8), promotion of fibroblast and neonatal epidermal basal cell proliferation (Figures 7 and 8), and elevation of antioxidant enzyme activity (Figure 9) compared with control groups, consistent with the wound healing properties of the majority of current plasma devices.

In terms of influencing the inflammatory process, previous reports indicate that plasma can induce the secretion of pro-inflammatory cytokines from neutrophils and macrophages[17,18] and the secretion of cytokines and growth factors from fibroblasts and keratinocytes,[18] thereby recruiting and activating inflammatory cells which further accelerate the process of debridement. In addition, plasma can reduce inflammatory damage by antagonising excessive oxidative stress through activation of the body's anti-oxidative stress protection mechanism, thereby accelerating wound healing.[13] Previous studies have shown that plasma significantly promotes angiogenesis[19-21] through the formation of NO, a major factor in angiogenesis[22,23] and the main active component of plasma.[24] Many studies have shown that plasma can promote the proliferation of keratinocytes,[18,25-27] thus enhancing epithelialization. Moreover, plasma can promote the deposition of collagen via accelerated collagen synthesis, evidenced by both in vitro and in vivo experiments.[13,28] Although the mechanisms and active components related to plasma that accelerate wound healing still require elucidation, the current view focuses on ROS and RNS, the principal active substances that are present in plasma.[5,9,29,30] The substantial formation of ROS and RNS (Figure 3) may explain the similar observations of

accelerated wound healing following the use of the new LTP device.

Interestingly, the hot-air group also demonstrated an acceleration of wound healing compared with the control group, especially in diabetic rats (Figure 5), suggesting that temperature is a substantial factor. Further cellular and molecular examination indicated that the promotion of wound healing by hot-air is due to the following: a reduction in inflammation (Figures 6 and 8), promotion of epithelialization (Figures 6 and 8), and elevation of TGF-β and antioxidant enzyme expression (Figures 8 and 9). In the present study, the temperature of the hot-air group was 43 ± 0.5°C, the same temperature of plasma reaching the skin. Although the temperature of the plasma in current devices usually ranges from 32°C[14] to 40°C,[13] it is higher than room temperature and should exhibit a thermal effect. However, current studies that focus on the acceleration of wound healing of plasma fail to also examine the role of temperature.

Previous studies have suggested that thermal effects can accelerate wound healing. Rabkin et al found that the local use of warm and moist heat packs on small experimental wounds in hospitalised patients increases local perfusion 3-fold greater than baseline values, raising oxygen tension by 39.5 mmHg from a baseline of 47.7 mmHg.[31] This has been further confirmed by another independent study.[32] It is well known that a principal factor in slow healing in diabetic wounds is poor blood circulation in these tissues, resulting in insufficient nutrients or oxygen in the wound closure region.[33] Local hyperthermia elevates tissue perfusion with sufficient nutrients and oxygen, playing an important role in diabetic wound healing. This may explain why the hot-air group demonstrated significant accelerated wound healing, especially in diabetic rats (Figure 5). Additionally, studies have demonstrated that thermal effects can control the number of bacteria and increase the number of fibroblasts.[31,34,35] Furthermore, another important effect of hyperthermia is the promotion of heat shock protein (HSP) expression.[36,37] HSPs have been demonstrated to have important roles in the reduction in inflammation and promotion of epithelialization, secretion of nitric oxide, and angiogenesis.[38-43] Consistent with this, in the present study, a number of these effects were also demonstrated in the hot-air group, such as a reduction in inflammation and promotion of epithelialization (Figures 6 and 8). Therefore, the heat released by the plasma device during treatment also played a positive role in wound healing, which cannot be ignored.

In particular, a comparison of the LTP and hot-air groups indicated that a number of the effects occurred only with the LTP device, such as neovascularisations and collagen deposition (Figures 7 and 8). Some effects were similar in both groups, such as elevation of antioxidant enzymes (Figures 8 and 9), while some of the effects of LTP were effective than that in the thermal group, such as a reduction in inflammation, elevation of TGF-β, and promotion of epithelialization (Figures 6 and 8). These results distinguished the effects of plasma from thermal effects, providing the basis for more in-depth investigation of plasma treatment in the medical field. However, it should be mentioned that a change in temperature is an aspect of plasma treatment that cannot be removed. Therefore, the acceleration of wound healing should be considered a combination of plasma-active substances and temperature effects.

In addition, although the new LTP device produces considerably more active substances in the plasma jet (data not shown), their concentration reaching the skin was not higher than in other reported plasma devices.[44] This may have resulted from the greater distance (8 cm versus 5 mm) or the different gas source. However, this does not influence its significantly accelerated effect on wound healing. Moreover, younger rats were used in the diabetic wound model (8-week-old), because streptozotocin (STZ) causes multiple deaths in rats older than 10-weeks. Younger rats have faster wound healing, so the duration of wound healing was considerably shorter in the diabetic wound model than the normal wound model. The corresponding thermal control group should be used to investigate the effects of plasma. Because the different plasma devices have different treatment temperatures, different thermal effects were observed.

5 | CONCLUSION

In summary, the new LTP device used in the present study has many advantages, such as a free gas source, long working distance, high gas flow rate, and large effective treatment area, which were effective in addressing the shortcomings of current plasma devices, greatly expanding the clinical and biomedical applications of plasma devices. In-depth wound healing experiments confirmed the efficacy of the new LTP device. In particular, the thermal control group was able to demonstrate thermal effects distinct from plasma effects, providing a valuable basis for a more in-depth investigation of plasma treatment for biomedical fields in the future.

ACKNOWLEDGEMENTS

This work was supported by the Yantai Healing Technology Co. Ltd.

CONFLICT OF INTEREST

The authors declare no conflicts of interest.

AUTHOR CONTRIBUTIONS

L.H., F.W., and Y. W. designed experiments, provided research funds, and finalised the manuscript; P. G., Y. L., J. L., N. Z., M. Z., Y. L., G. Z., N. W., and A.W. performed experiments and analysed the data; P. G. and Y. L. co-wrote the manuscript. All contributing authors agree to the publication of this article.

DATA AVAILABILITY STATEMENT

Research data are not shared.

REFERENCES

1. Vonw T, Schmidt A, Bekeschus S, Wende K, Weltmann KD. Plasma medicine: a field of applied redox biology. *In Vivo*. 2019;33(4):1011-1026. https://doi.org/10.21873/invivo.11570
2. Heinlin J, Isbary G, Stolz W, et al. Plasma applications in medicine with a special focus on dermatology. *J Eur Acad Dermatol Venereol*. 2011;25(1):1-11. https://doi.org/10.1111/j.1468-3083.2010.03702.x
3. Izadjoo M, Zack S, Kim H, Skiba J. Medical applications of cold atmospheric plasma: state of the science. *J Wound Care*. 2018;27(Sup9):S4-s10. https://doi.org/10.12968/jowc.2018.27.Sup9.S4
4. Laroussi M. Sterilization of contaminated matter with an atmospheric pressure plasma. *IEEE Trans Plasma Sci*. 1996;24(3):1188-1191.
5. Gan L, Zhang S, Poorun D, et al. Medical applications of non-thermal atmospheric pressure plasma in dermatology. Journal der Deutschen Dermatologischen Gesellschaft =. *J German Soc Dermatol*. 2018;16(1):7-13. https://doi.org/10.1111/ddg.13373
6. Gherardi M, Tonini R, Colombo V. Plasma in dentistry: brief history and current status. *Trends Biotechnol*. 2018;36(6):583-585. https://doi.org/10.1016/j.tibtech.2017.06.009
7. Zubor P, Wang Y, Liskova A, et al. Cold atmospheric pressure plasma (CAP) as a new tool for the management of vulva cancer and vulvar premalignant lesions in gynaecological oncology. *Int J Mol Sci*. 2020;21(21):7988. https://doi.org/10.3390/ijms21217988
8. Bekeschus S, Schmidt A, Weltmann K-D, von Woedtke T. The plasma jet kINPen – a powerful tool for wound healing. *Clin Plasma Med*. 2016;4(1):19-28. https://doi.org/10.1016/j.cpme.2016.01.001
9. Weltmann KD, Kindel E, Brandenburg R, et al. Atmospheric pressure plasma jet for medical therapy: plasma parameters and risk estimation. *Contrib Plasma Physics*. 2009;49(9):631-640. https://doi.org/10.1002/ctpp.200910067
10. Bernhardt T, Semmler ML, Schafer M, Bekeschus S, Emmert S, Boeckmann L. Plasma medicine: applications of cold atmospheric pressure plasma in dermatology. *Oxid Med Cell Longev*. 2019;2019:3873928. https://doi.org/10.1155/2019/3873928
11. Brehmer F, Haenssle HA, Daeschlein G, et al. Alleviation of chronic venous leg ulcers with a hand-held dielectric barrier discharge plasma generator (PlasmaDerm([R]) VU-2010): results of a monocentric, two-armed, open, prospective, randomized and controlled trial (NCT01415622). *J Eur Acad Dermatol Venereol*. 2015;29(1):148-155. https://doi.org/10.1111/jdv.12490
12. Varghese F, Bukhari AB, Malhotra R, De A. IHC profiler: an open source plugin for the quantitative evaluation and automated scoring of immunohistochemistry images of human tissue samples. *PLoS One*. 2014;9(5):e96801. https://doi.org/10.1371/journal.pone.0096801
13. Arndt S, Schmidt A, Karrer S, von Woedtke T. Comparing two different plasma devices kINPen and Adtec SteriPlas regarding their molecular and cellular effects on wound healing. *Clin Plasma Med*. 2018;9:24-33. https://doi.org/10.1016/j.cpme.2018.01.002
14. Mirpour S, Fathollah S, Mansouri P, et al. Cold atmospheric plasma as an effective method to treat diabetic foot ulcers: a randomized clinical trial. *Sci Rep*. 2020;10(1):10440. https://doi.org/10.1038/s41598-020-67232-x
15. Shimizu T, Steffes B, Pompl R, et al. Characterization of microwave plasma torch for decontamination. *Plasma Processes Polym*. 2008;5(6):577-582. https://doi.org/10.1002/ppap.200800021
16. Reuter S, von Woedtke T, Weltmann K-D. The kINPen—a review on physics and chemistry of the atmospheric pressure plasma jet and its applications. *J Phys D Appl Phys*. 2018;51(23):233001. https://doi.org/10.1088/1361-6463/aab3ad
17. Kaushik NK, Kaushik N, Adhikari M, et al. Preventing the solid cancer progression via release of anticancer-cytokines in co-culture with cold plasma-stimulated macrophages. *Cancer*. 2019;11(6):842. https://doi.org/10.3390/cancers11060842
18. Arndt S, Landthaler M, Zimmermann JL, et al. Effects of cold atmospheric plasma (CAP) on ß-defensins, inflammatory cytokines, and apoptosis-related molecules in keratinocytes in vitro and in vivo. *PLoS One*. 2015;10(3):e0120041. https://doi.org/10.1371/journal.pone.0120041
19. Duchesne C, Banzet S, Lataillade JJ, Rousseau A, Frescaline N. Cold atmospheric plasma modulates endothelial nitric oxide synthase signalling and enhances burn wound neovascularisation. *J Pathol*. 2019;249(3):368-380. https://doi.org/10.1002/path.5323
20. Arndt S, Unger P, Berneburg M, Bosserhoff AK, Karrer S. Cold atmospheric plasma (CAP) activates angiogenesis-related molecules in skin keratinocytes, fibroblasts and endothelial cells and improves wound angiogenesis in an autocrine and paracrine mode. *J Dermatol Sci*. 2018;89(2):181-190. https://doi.org/10.1016/j.jdermsci.2017.11.008
21. Miller V, Lin A, Kako F, et al. Microsecond-pulsed dielectric barrier discharge plasma stimulation of tissue macrophages for treatment of peripheral vascular disease. *Phys Plasmas*. 2015;22(12):122005. https://doi.org/10.1063/1.4933403
22. Kapila V, Sellke FW, Suuronen EJ, Mesana TG, Ruel M. Nitric oxide and the angiogenic response: can we improve the results of therapeutic angiogenesis? *Expert Opin Investig Drugs*. 2005;14(1):37-44. https://doi.org/10.1517/13543784.14.1.37
23. Nichols SP, Storm WL, Koh A, Schoenfisch MH. Local delivery of nitric oxide: targeted delivery of therapeutics to bone and connective tissues. *Adv Drug Deliv Rev*. 2012;64(12):1177-1188. https://doi.org/10.1016/j.addr.2012.03.002
24. Isbary G, Morfill G, Schmidt HU, et al. A first prospective randomized controlled trial to decrease bacterial load using cold atmospheric argon plasma on chronic wounds in patients. *Br J Dermatol*. 2010;163(1):78-82. https://doi.org/10.1111/j.1365-2133.2010.09744.x
25. Schmidt A, von Woedtke T, Bekeschus S. Periodic exposure of keratinocytes to cold physical plasma: an in vitro model for redox-related diseases of the skin. *Oxid med Cell Longev*. 2016;2016:9816072. https://doi.org/10.1155/2016/9816072

26. Schmidt A, Bekeschus S, Wende K, Vollmar B, von Woedtke T. A cold plasma jet accelerates wound healing in a murine model of full-thickness skin wounds. *Exp Dermatol*. 2017;26(2):156-162. https://doi.org/10.1111/exd.13156
27. Hasse S, Duong Tran T, Hahn O, et al. Induction of proliferation of basal epidermal keratinocytes by cold atmospheric-pressure plasma. *Clin Exp Dermatol*. 2016;41(2):202-209. https://doi.org/10.1111/ced.12735
28. Arndt S, Unger P, Wacker E, et al. Cold atmospheric plasma (CAP) changes gene expression of key molecules of the wound healing machinery and improves wound healing in vitro and in vivo. *PLoS One*. 2013;8(11):e79325. https://doi.org/10.1371/journal.pone.0079325
29. Schmidt A, Bekeschus S. Redox for repair: cold physical plasmas and Nrf2 signaling promoting wound healing. *Antioxidants*. 2018;7(10):146. https://doi.org/10.3390/antiox7100146
30. Schmidt A, Wende K, Bekeschus S, et al. Non-thermal plasma treatment is associated with changes in transcriptome of human epithelial skin cells. *Free Radic Res*. 2013;47(8):577-592. https://doi.org/10.3109/10715762.2013.804623
31. Rabkin JM, Hunt TK. Local heat increases blood flow and oxygen tension in wounds. *Arch Surg*. 1987;122(2):221-225. https://doi.org/10.1001/archsurg.1987.01400140103014
32. Ikeda T, Tayefeh F, Sessler DI, et al. Local radiant heating increases subcutaneous oxygen tension. *Am J Surg*. 1998;175(1):33-37. https://doi.org/10.1016/s0002-9610(97)00237-7
33. Paneni F, Beckman JA, Creager MA, Cosentino F. Diabetes and vascular disease: pathophysiology, clinical consequences, and medical therapy: part I. *Eur Heart J*. 2013;34(31):2436-2443. https://doi.org/10.1093/eurheartj/eht149
34. Lee ES, Caldwell MP, Talarico PJ, Kuskowski MA, Santilli SM. Use of a noncontact radiant heat bandage and *Staphylococcus aureus* dermal infections in an ovine model. *Wound Repair Regen*. 2000;8(6):562-566. https://doi.org/10.1046/j.1524-475x.2000.00562.x
35. Xia Z, Sato A, Hughes MA, Cherry GW. Stimulation of fibroblast growth in vitro by intermittent radiant warming. *Wound Repair Regen*. 2000;8(2):138-144. https://doi.org/10.1046/j.1524-475x.2000.00138.x
36. Wilson N, McArdle A, Guerin D, et al. Hyperthermia to normal human skin in vivo upregulates heat shock proteins 27, 60, 72i and 90. *J Cutan Pathol*. 2000;27(4):176-182. https://doi.org/10.1034/j.1600-0560.2000.027004176.x
37. Hintzsche H, Riese T, Stopper H. Hyperthermia-induced micronucleus formation in a human keratinocyte cell line. *Mutat Res*. 2012;738-739:71-74. https://doi.org/10.1016/j.mrfmmm.2012.08.004
38. Matsuda M, Hoshino T, Yamashita Y, et al. Prevention of UVB radiation-induced epidermal damage by expression of heat shock protein 70. *J Biol Chem*. 2010;285(8):5848-5858. https://doi.org/10.1074/jbc.M109.063453
39. Crowe J, Aubareda A, McNamee K, et al. Heat shock protein B1-deficient mice display impaired wound healing. *PLoS One*. 2013;8(10):e77383. https://doi.org/10.1371/journal.pone.0077383
40. Laplante AF, Moulin V, Auger FA, et al. Expression of heat shock proteins in mouse skin during wound healing. *J Histochem Cytochem*. 1998;46(11):1291-1301. https://doi.org/10.1177/002215549804601109
41. Pritchard KA Jr, Ackerman AW, Gross ER, et al. Heat shock protein 90 mediates the balance of nitric oxide and superoxide anion from endothelial nitric-oxide synthase. *J Biol Chem*. 2001;276(21):17621-17624. https://doi.org/10.1074/jbc.C100084200
42. Duval M, Le Boeuf F, Huot J, Gratton JP. Src-mediated phosphorylation of Hsp90 in response to vascular endothelial growth factor (VEGF) is required for VEGF receptor-2 signaling to endothelial NO synthase. *Mol Biol Cell*. 2007;18(11):4659-4668. https://doi.org/10.1091/mbc.e07-05-0467
43. Bruns AF, Yuldasheva N, Latham AM, et al. A heat-shock protein axis regulates VEGFR2 proteolysis, blood vessel development and repair. *PLoS One*. 2012;7(11):e48539. https://doi.org/10.1371/journal.pone.0048539
44. Cheng KY, Lin ZH, Cheng YP, et al. Wound healing in Streptozotocin-induced diabetic rats using atmospheric-pressure argon plasma jet. *Sci Rep*. 2018;8(1):12214. https://doi.org/10.1038/s41598-018-30597-1

SUPPORTING INFORMATION

Additional supporting information may be found online in the Supporting Information section at the end of this article.

How to cite this article: Guo P, Liu Y, Li J, et al. A novel atmospheric-pressure air plasma jet for wound healing. *Int Wound J*. 2022;19(3):538-552. https://doi.org/10.1111/iwj.13652